PRINT ISSN 1119-8362
Electronic ISSN 2659-1502

Full-text Available Online at
https://www.ajol.info/index.php/jasem
http://www.bioline.org.br/ja

J. Appl. Sci. Environ. Manage.
Vol. 27 (8) 1645-1650 August 2023

Statistical Optimization of Faujasite Zeolite Synthesis from Bauxite Alumina and Rice Husk Silica

***[1]OSHOMOGHO, FO; [2]UJILE, AA; [2]DAGDE, KK; [2]EHIRIM, EO**

*[*1]Department of Chemical Engineering, University of Benin, Benin City, Edo Sate, Nigeria*
[2]Department of Chemical/Petrochemical, Rivers State University, Nkpolu-Oroworuko, Rivers State, Port Harcourt, Nigeria

**Corresponding Author Email: fred.oshomogho@uniben.edu, Tel: +2348055966268*
Co-Author Email: Ujile.awajiogak@ust.edu.ng; dagde.kenneth@ust.edu.ng; ehirim.emmanuel@ust.edu.ng

ABSTRACT: Faujasite, a molecular sieve zeolite Y aluminosilicate mineral, has excellent catalytic strength and is employed in various industries. The study therefore, seek to synthesize a faujasite zeolite with a hydrothermal treatment of local clay alumina and rice husk silica using central composite design (CCD) of experiment in response surface methodology (RSM) in a 1000ml 2-neck flat bottom flask on a constant temperature magnetic stirrer at 120^{o}C for 6 hours. SiO_2, Al_2O_3, and NaOH were coded at three levels at various masses and Si/Al mole ratios. A significant model with an F-value of 142.27 and a Predicted R^2 of 0.9558 was developed using statistically optimized hydrothermal synthesis. 3.07g NaOH, 10.50g SiO2, and 2.61g Al2O3 were needed to synthesize FAU zeolite with Si/Al mole ratio > 2. At 1095.8cm^{-1} in IR spectrum, silicone (Si – O – Si) was the most abundant functional group in the zeolite. EDS and XRD revealed a faujasite zeolite-Y with 85.60wt% Si and 17.50wt% Al. Octahedral modified zeolite Y crystals were seen in SEM topography. At low relative pressures (P/P0 < 0.056), BET showed significant N_2 absorption, indicating micropores. The zeolite's BET study indicated a specific surface area of 1750.0m^2/g and a pore diameter of 1.847nm. Transesterification of high-free fatty acid triglycerides can be catalyzed by microporous faujasite zeolite.

DOI: https://dx.doi.org/10.4314/jasem.v27i8.6

Cite this paper as: OSHOMOGHO, F. O; UJILE, A. A; DAGDE, K. K; EHIRIM, E. O. (2023). Statistical Optimization of Faujasite Zeolite Synthesis from Bauxite Alumina and Rice Husk Silica. *J. Appl. Sci. Environ. Manage.* 27 (8) 14-1650

Dates: Received: 10 July 2023; Revised: 25 July 2023; Accepted: 14 August 2023 Published: 30 August 2023

Keywords: Faujasite, Zeolite, Silica, Alumina, Hydrothermal

Clay materials have been used to synthesize zeolites because of their fundamental components (Murray 2002). Because the physical and chemical properties of the products vary depending on the thermal or chemical treatment of the feedstock clay materials (Kumar 2013), zeolites of varying types have been used for applications in a wide range of catalytic functions. Regular intracrystalline cavities and channels with atomic-scale dimensions are created when SiO_4 and AlO_4 tetrahedra are linked by sharing an oxygen atom. Hydrated aluminosilicate zeolites have porous three-dimensional frameworks and are classified as hydrated crystalline materials. In the hydrothermal process, natural deposits rich in silica, alumina, cations, and water are transformed into zeolite. Natural resources in Nigeria include kaolin clay and other silica-containing minerals (Badmus and Olatinsu 2009). It has been proven that distinct zeolites can be formed from the same gel mixture using different silica species. Commercially available forms of silica used in zeolite production include solutions, gels, fumed solids, colloids, and organic derivatives such tetra-ethyl-orthosilicate (Prasetyoko et al. 2006). You can also use silica-containing plants in the synthesis of zeolite (Pandiangan et al. 2019). Because zeolites have a consistent pore structure and their surface can be hydrophobic, they offer a distinct advantage over other solid heterogeneous catalysts

**Corresponding Author Email: fred.oshomogho@uniben.edu*

when it comes to their employment in industrial applications (Kosinov and Hensen 2020). This advantage allows them to prevent the deactivation of the catalyst's active sites by polar solvents such as water or alcohol. Synthesizing zeolite is an effective strategy for overcoming a number of constraints brought on by diffusion, which can significantly improve optimal output in transesterification reactions (Derbe *et al.* 2021). Because of the high reactivity of zeolite catalyst, it possesses a tremendous potential for catalysis. Hence, objective of this paper was hydrothermal synthesis of faujasite zeolite-Y with local clay alumina and rice husk silica using central composite design (CCD) of experiment in response surface methodology (RSM)

MATERIAL AND METHODS

The major material materials used in this study were aluminium containing clay sample from Ikpeshi community in Akoko-Edo local government area of Edo State. Rice husk was collected as waste in a local rice mill in Ekperi community in Etsako central local government area of Edo state. The clay sample was dug from the ground at a dept of about 10cm to avoid organic materials contamination at the surface of the soil.

Extraction of Silica from RH: 200g of rice husk was fed to a muffle furnace with a crucible and lid and burned at 700oC for 3 hours to produce pinkish white ash and compute the ash content. A 1000ml round bottom flask containing 20g of oven-dried ash and 300ml of 2.5M NaOH solution was boiled for 15 minutes under complete reflux on a heating mantle. After cooling to room temperature, the mixture was filtered using whiteman's No 11 filter paper. The filtrate was carefully added conc. H_2SO_4 with steady glass rod stirring till pH 7, at which the silica content got crystalized completely as white precipitates. Thus, the precipitates were filtered, washed, and dried at 105^{o}C. An EDXRF-equipped X-ray fluorescence examined the dried sample for percentage silica content. Experiment reaction is represented by equation (1) and (2):

$$Ash + 2NaOH \xrightarrow[heat]{} Na_2SiO_3 + H_2O \quad (1)$$

$$Na_2SiO_3 + H_2SO_4 \xrightarrow[heat]{} SiO_2 + Na_2SO_4 + H_20 \quad (2)$$

Alumina Extraction: The Bayer Process was used in the extraction of alumina from clay according to Tantawy and Ali Alomari (2019). The rocky clay sample was crushed mechanically and sieved at 100 µm. The acid leaching process was performed in a round-bottom flask on a magnetic stirrer set to a high temperature. All metals in the sample were first converted to oxides by calcining the sample at 900°C for 240 minutes. To completely dissolve the aluminum and iron in the clay sample, about 100g of the crushed and calcined sample was added enough amount of 25% HCl solution and then placed in an autoclave where it was heated for 150minutes. The silica (Si-stoff)-dominated solid residue could be easily extracted. The solution's pH was brought up to around 12–13 by adding NaOH pellets. Once again, this went into an autoclave and was subjected to high heat and pressure for roughly 120 minutes. For around 2 hours, the solid residue was dried in an electric air-drying oven set to 110 degrees Celsius after being cleaned with distilled water. Alumina will be separated from the solutions by filtration, washing, and drying in an oven set to 105 degrees Celsius. Energy dispersive X-ray fluorescence (EDXRF) analysis was used to determine the purity of the produced alumina. The reaction for the experiment is:

$$Al_2O_3.3H_2O + 2NaOH \frac{250^oC}{High\ Pressure} 2NaAlO_2 + 4H_2O \quad (3)$$

$$2NaAlO_2 + H_2O \rightarrow 2NaOH + Al_2O_3 \quad (4)$$

Optimization of Zeolite Synthesis from Alumina and Silica: The experiment was set up using a Central Composite Design (CCD) with three factors. Response surface approach was used to optimize the results. The optimized factors' silica, alumina, and sodium hydroxide masses were each represented by a three-level. Central Composite Design (CCD) (Ebrahimi-Najafabadi et al. 2014)was used with the aid of Design-Expert version 13.0.6 to implement a response surface methodology (RSM). There was a total of 20 experimental runs with three independent variables: three factorial points, three axial points, and six replicates at the center point.

RESULTS AND DISCUSSION

The Analysis of Variance (ANOVA) for the Quadratic Model: The F-value of 146.27 in Table 1 illustrates the significance of the model. The probability of observing an F-value this high due to noise is little more than 0.01%. A model term is statistically significant if its p-value is less than 0.0500. Model terms that are particularly relevant here include A, B, C, AB, AC, BC, A_2, B_2, and C_2.

An unimportant model term is one with a value larger than 0.1000. It may be beneficial to execute a model reduction if the model has a high number of unnecessary terms (other than those required to support hierarchy). Lack of Fit F-value = 2.13 is not statistically significant when compared to the pure

error. There is a 21.33 percent chance that the high Lack of Fit F-value was due to chance alone (Casler 2015). It's preferable to have a lack of fit that isn't statistically significant.

Table 1: The ANOVA for Quadratic Model

Source	Sum of Squares	df	Mean Square	F-value	p-value
Model	165.83	9	18.43	146.27	< 0.0001
A-Mass of SiO_2	9.64	1	9.64	76.49	< 0.0001
B-Mass of Al_2O_3	3.86	1	3.86	30.68	0.0002
C-Mass of NaOH	13.00	1	13.00	103.17	< 0.0001
AB	2.30	1	2.30	18.25	0.0016
AC	3.08	1	3.08	24.45	0.0006
BC	1.05	1	1.05	8.36	0.0161
A^2	38.89	1	38.89	308.71	< 0.0001
B^2	10.60	1	10.60	84.11	< 0.0001
C^2	102.03	1	102.03	809.93	< 0.0001
Residual	1.26	10	0.1260		
Lack of Fit	0.8571	5	0.1714	2.13	0.2133

The Fit Statistics: A comparison of the Predicted R^2 of 0.9558 and the Adjusted R^2 of 0.9857 reveals a small difference (less than 0.2) between the two values (Table 2). Adequate Precision employs the signal-to-noise ratio as a metric. A ratio greater than 4 is preferred. The ratio of signal to noise is 36.524, which is good. This model can be used to test out various layout options.

Table 2 The Fit Statistics

R^2	0.9925
Adjusted R^2	0.9857
Predicted R^2	0.9558
Adequate Precision	36.5240
Std. Deviation	0.3549
Mean	5.70
C.V. %	6.22

Final Equation in Terms of Coded Factors: For a fixed concentration of each coded component, the appropriate equation can be used to predict the reaction. Assigning a value of +1 to a high level of a factor and a value of -1 to a low level is the default choice. The relative weights of the components can be calculated using the encoded equation (equation 5) by comparing the factor coefficients.

$$\text{Si/Al Mole Ratio} = 9.23 + 0.8400A + 0.5319B + 0.9755C + 0.5360AB + 0.6205AC - 0.3628BC - 1.64A^2 - 0.8574B^2 - 2.66C^2 \quad (5)$$

Response Surface Plots of Zeolite Synthesis: Figure 1 displays the outcomes of the optimization of hydrothermal zeolite synthesis. Based on the results of the aluminum to silica mole ratio interaction, the best molar silica concentration is around 10 mole to 3 mole of aluminum. The acidity and structural integrity of the resulting zeolite can be fine-tuned by adjusting the initial composition. The zeolite's crystal size and morphology can also be affected by the kind and concentration of the alkali metal or alkaline earth metal hydroxides. Similar to how a low mole ratio of SiO_2 causes less silica crystallization, a high mole ratio of SiO_2 or Al_2O_3 causes less crystallization of the necessary faujasite zeolite. It has been reported that the crystal size and morphology of zeolite synthesized via the hydrothermal process are affected by the kind and concentration of the alkali metal or alkaline earth metal hydroxides. The zeolite crystallization type was significantly affected by the NaOH concentration, as shown in Figure 2

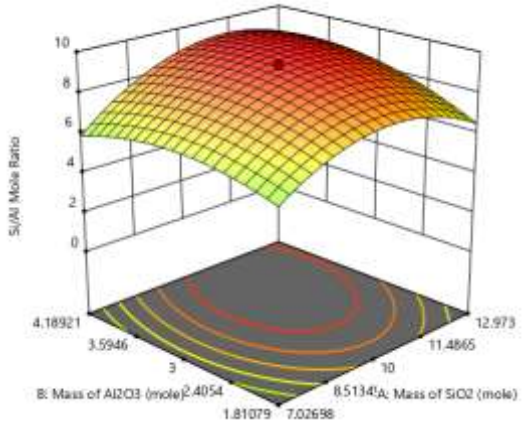

Fig 1: Response surface interaction of masses of SiO_2 vs Al_2O_3 on mole ratio of Si/Al on zeolite

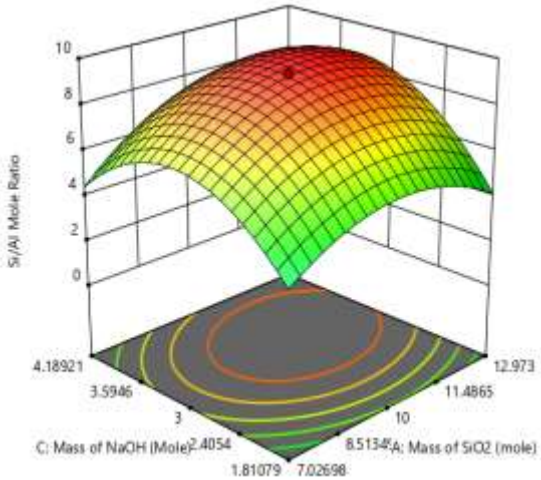

Fig 2 Response surface interaction of masses of SiO_2 versus NaOH on mole ratio of Si/Al on zeolite

Optimum results of RSM Zeolite Synthesis: It has been reported that the type and concentration of the alkali metal or alkaline earth metal hydroxides used in the hydrothermal synthesis of zeolite affect the crystal size and shape of the resulting material. Figure 4 demonstrates that the concentration of NaOH had a major impact on the zeolite crystallization type.

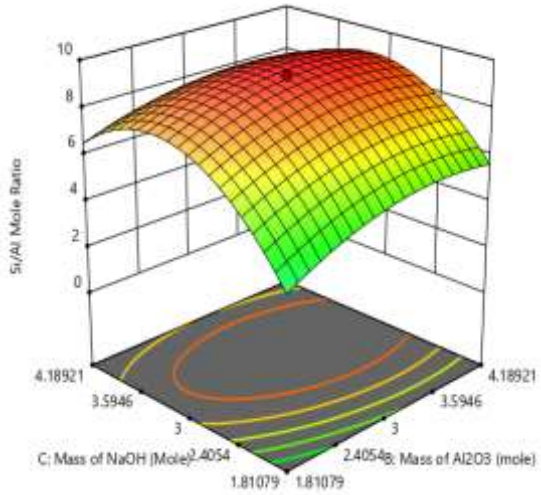

Fig 3 Response surface interaction of masses of Al_2O_3 versus NaOH on mole ratio of Si/Al on zeolite

XRD Analysis of Synthesized Zeolite: Lattice spacing analysis by X-ray diffraction shows that the synthesized zeolite is quite similar to that of pure faujasite (Frising and Leflaive 2008). XRD patterns showed that faujasite zeolite-X was formed in the presence of sodalite. The crystallinity of the faujasite zeolite catalyst was determined with the use of an X-ray diffractometer. The XRD spectrum of a zeolite catalyst that was manufactured optimally with different amounts of Ce is shown in Figure 5. A very prominent peak can be seen in the spectrum of the sample at 2 = 24.81 degrees, which is often associated with the formation of amorphous SiO_2. In addition, there are three faint peaks at 2 = 23.499°, 14.41°, and 30.132°. Each oxygen atom is shared by two tetrahedra microporous structures, and this structure is supported by these peaks, as is typical of sodalite materials.

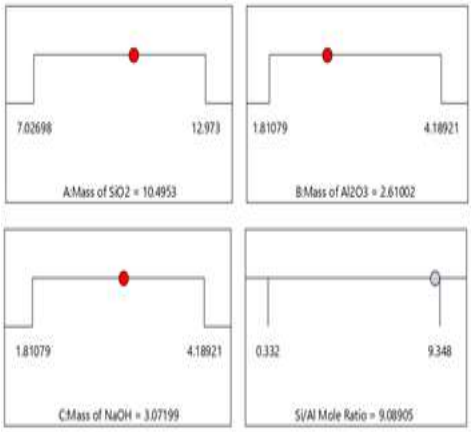

Fig 4 Results of optimal condition of zeolite synthesis

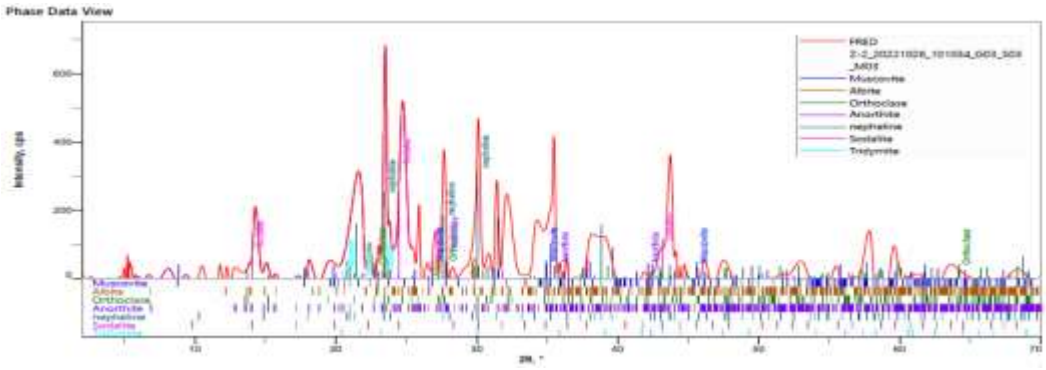

Fig 5 XRD Spectrum of synthesized catalyst

SEM of Synthesized Zeolite: SEM images of zeolite reveal clear particles with a 2D particle shape resembling a fuzzy disk (Figure 6, different magnifications). The zeolite meets the requirements of the American Petroleum Institute's standard for molecular sieves, as shown by microscopy study of its particle morphologies. The crystalline structure of the modified zeolite Y was octahedral, as shown by the topography of the sample obtained using scanning electron microscopy (SEM). The particle size distribution of zeolite Y is very even, with particles ranging in size from 1 to 3nm on average (Ordóñez and Díaz 2009). The unit cell of the imperfect particles has a rough and imperfect surface. Hydrothermal reactions can leave some aluminosilicate ions adsorbed on particle surfaces if not all aluminosilicate ions dissolve in water. It's also possible that unburned Na impurities in the mother liquor are to fault (Novembre et al. 2011).

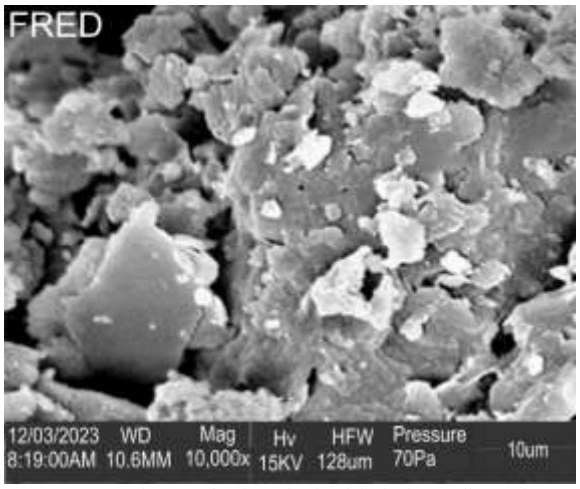

Fig 6 SEM micrograph of synthesized faujasite zeolite at three magnifications of 10000x.

EDS Analysis of Modified Faujasite Zeolite: Energy dispersive X-ray spectrometer was used to determine the Si/Al ratio in the modified zeolite catalyst. Figure 7 revealed that Si was resent at 85.60wt% and Al at 17.50wt% making a ratio of 4.891. This is a faujasite type of zeolite and a zeolite Y which usually have ratio Si/Al >2 (Ajayi, Adefila, and Ityokumbul 2018). Stability of zeolite is enhanced with an increase in the Si/Al ratio (García-Martínez, Li and Krishnaiah, 2012; Mgbemere et al., 2019).

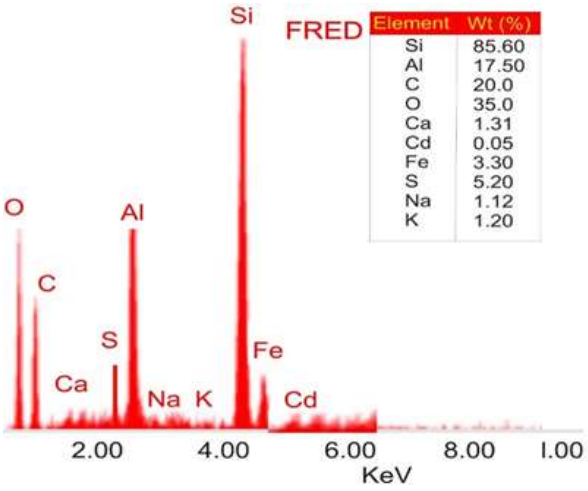

Fig 7: EDS spectrum of synthesized faujasite zeolite

Conclusion: Zeolite was synthesized from Ikpeshi clay, Edo state, Nigeria. This work demonstrated the development of a hydrothermal process to produce an important industrial catalyst from clay and rice husk silica. Sodium hydroxide doping of rice husk silica and aluminosilicate containing clay yielded a faujasite zeolite. The analysis of variance showed model terms were significance. The obtained optimum conditions showed that a faujasite zeolite Y type was obtained from the results of characterizations conducted.

REFERENCES*

Ajayi, O. A., Adefila, S. S., & Ityokumbul, M. T. (2018). Monitoring zeolite NaY formation from potassium-rich Nigerian kaolinite clay. *Ain Shams Engin J*, *9*(4), 1653–1661.

Badmus, B. S., & Olatinsu, O. B. (2009). Geophysical evaluation and chemical analysis of kaolin clay deposit of Lakiri village, Southwestern Nigeria. *Intern. J. of Phy. Sci*, *4*(10), 592–606.

Casler, MD. (2015). Fundamentals of Experimental Design: Guidelines for Designing Successful Experiments. *Agronomy J.* 107(2):692.

Derbe, T; Shewaye T; and Mamaru B; (2021). A Short Review on Synthesis, Characterization, and Applications of Zeolites. *Adv in Mater. Sci. and Engineering* 2021.

Ebrahimi-Najafabadi, H; Leardi, R and Jalali-Heravi, M. (2014). Experimental Design in Analytical Chemistry -Part I: Theory. *J. of AOAC Intern.* 97(1):3–11.

Frising, T. and Leflaive, P. (2008). Extraframework Cation Distributions in X and Y Faujasite Zeolites: A Review. *Microporous and Mesoporous Mater.*, 114:27–63.

García-Martínez, JKL, and Gautham K. (2012). A Mesostructured Y Zeolite as a Superior FCC Catalyst – from Lab to Refinery. *Chem. Com.* 48(97):11841–43.

Kosinov, N. and Hensen EJM. (2020). Reactivity, Selectivity, and Stability of Zeolite-Based Catalysts for Methane Dehydroaromatization. *Advan. Mater* 32(44).

Kumar, S. (2013). Enzymatic Transesterification of Waste Animal Fats for Production of Biodiesel. 1-166

Mgbemere, HE; Ikenna CE; Ganiyu L; Ovri H. and Chaudhary AL. (2019). Preparation and Characterization of Zeolite Type 4A Using Kaolin from Ajebo, Nigeria. *Pertanika J. of Sci and Tech.* 27(4):2427–38.

Murray, H. (2002). Industrial Clays Case Study. *Min, Miner. and Sust. Dev.* 1(64):1–9.

Novembre, D; di-Sabatino, B; Gimeno, D. and Pace, C. (2011). Synthesis and Characterization of Na-X, Na-A and Na-P Zeolites and Hydroxysodalite from Metakaolinite. *Clay Min.* 46(3):339–54.

Ordóñez, S. and Díaz, E. (2009). Basic Zeolites: Structure, Preparation and Environmental Applications. *Handbook of Zeolites: Stru., Prop. and Appl.* 2009:51–66.

Pandiangan, KD; Simanjuntak, W; Pratiwi, E. and Rilyanti, M. (2019). Characteristics and Catalytic Activity of Zeolite-a Synthesized from Rice Husk Silica and Aluminium Metal by Sol-Gel Method. *J. of Phy: Confer. Series* 1338(1).

Prasetyoko, D; Ramli, Z; Endud, S; Hamdan, H. and Sulikowski, B. (2006). Conversion of Rice Husk Ash to Zeolite Beta. *Waste Manage.* 26(10):1173–79.

Tantawy, MA and Alomari, AA. (2019). Extraction of Alumina from Nawan Kaolin by Acid Leaching. *Orient. J. of Chem.* 35(3):1013–21.